

Cyclometalation of Secondary Benzyl Amines by Ruthenium(II) Complexes

Jean-Baptiste Sortais,[†] Nicolas Pannetier,[†] Nicolas Clément,[†] Laurent Barloy,^{*,†}
Claude Sirlin,[†] Michel Pfeffer,^{*,†} and Nathalie Kyritsakas[‡]

Institut de Chimie de Strasbourg, Université Louis Pasteur, Laboratoire de Synthèses Métallo-Induites and Service Commun des Rayons X, CNRS, UMR 7177, 4 rue Blaise Pascal, 67000 Strasbourg, France

Received October 23, 2006

The cyclometalation of chiral secondary amines through *ortho*-metalation of an aryl group occurred readily with $[(\eta^6\text{-benzene})\text{RuCl}_2]_2$ in acetonitrile. Reasonable to good yields of the expected cationic products of the form $[(\eta^6\text{-benzene})\text{Ru}(\text{N}-\text{C})(\text{NCMe})](\text{PF}_6)$, in which N–C represents the cyclometalated ligands, were obtained with bis-(*R*)-phenylethylamine, bis-(*R*)-1-naphthylethylamine, and (2*R*,5*R*)-2,5-diphenylpyrrolidine. Variable proportions of the expected four diastereoisomers were found according to NMR studies. The stereochemistry of complexes was investigated by 2D NMR in solution and by X-ray diffraction of single crystals. The (*S*) configuration at the metal was generally associated with a δ conformation of the metallacycle, and conversely, the (*R*) configuration with the λ conformation.

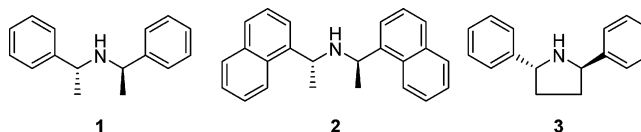
Introduction

We have recently investigated the use of cycloruthenated complexes as potential catalyst precursors for the catalytic transfer hydrogenation of prochiral ketones.¹ We have indeed found that organoruthenium compounds obtained with chiral primary and secondary amines cycloruthenated via the intramolecular CH activation at an *ortho* position of an aromatic ring displayed good catalytic properties for this reaction, as excellent activities (TON > 30 × 10³) and good to excellent selectivities (ee up to 90%) were observed.² We have also found that the catalytic performances of cycloruthenated compounds obtained with secondary amines were superior to those of primary amines. In this paper we disclose the cycloruthenation of secondary amines and the full characterization of the formed compounds, which display significant structural differences with corresponding primary amine derivatives. As these amines are built up with two chiral ArCHMe– groups (Ar = phenyl, naphthyl) attached to the NH unit, besides the two chiral carbon atoms, the other chiral centers of the molecules are the ruthenium and the nitrogen atoms.

Results and Discussion

Synthesis. We have limited our choice to three C₂-symmetric chiral secondary amines (Chart 1), in order to restrict the number of possible isomers derived from their cycloruthenation.³ The absolute configuration of both asymmetric carbon atoms of each amine is (*R*). The cycloruthenation conditions were the same as those that had been optimized for benzylic primary amines⁴

Chart 1. Benzylic Amines



(Scheme 1): the chiral amines were treated with 1 equiv of $[\text{Ru}(\eta^6\text{-C}_6\text{H}_6)\text{Cl}_2]_2$ in acetonitrile with an excess of sodium hydroxide and potassium hexafluorophosphate at room temperature.⁵ NMR monitoring of the reaction showed that the secondary amines were not completely converted into the cycloruthenated complexes after 3 days, by contrast with the unhindered primary amines, for which conversion was 100%.⁴ Indeed, the conversions reached 70%, 10%, and 90%, respectively, for complexes 4–6 (Chart 2); the conversion of the very hindered amine 2 into complex 5 could be increased to 27% by allowing the reaction to run for 21 days. Complexes 4–6 were purified by column chromatography over alumina and isolated with 65%, 23%, and 85% respective yields.

Fortunately, the unreacted amines remained free and could be easily recovered by extraction with pentane, which is a valuable result for processes involving costly chiral ligands. This result contrasts with the cycloruthenation of primary amines, for which an excess of ligand led to ruthenacyclic complexes with two amines, one being N–C-chelated and the second N-coordinated to Ru. It is probable that the steric hindrance of secondary amines prevents such a side reaction. For this reason, we expected that it would not be necessary to use a large excess of ruthenium source in the cycloruthenation process; however, running the reaction with a 2:1 instead of 1:1 (amine 1)/ $[\text{Ru}(\eta^6\text{-C}_6\text{H}_6)\text{Cl}_2]_2$ ratio led to a very low conversion (10%) after 3 days at RT. Eventually, complex 4 was converted into 7 in good yields (80%) through addition of an excess of dimethylphenylphosphine (Scheme 2).

(4) Sortais, J. B.; Pannetier, N.; Holuigue, A.; Barloy, L.; Sirlin, C.; Pfeffer, M.; Kyritsakas, N. *Organometallics* 2007, 26, XXXX om060973t.

(5) Applying the standard cycloruthenation conditions of tertiary amines (see: Fernandez, S.; Pfeffer, M.; Rittleng, V.; Sirlin, C. *Organometallics* 1999, 18, 2390–2394) to our secondary amines, i.e., heating to 45 °C, did not lead to any improvement of the chemical yields.

* Corresponding authors. E-mail: pfeffer@chimie.u-strasbg.fr; barloy@chimie.u-strasbg.fr.

[†] Laboratoire de Synthèses Métallo-Induites.

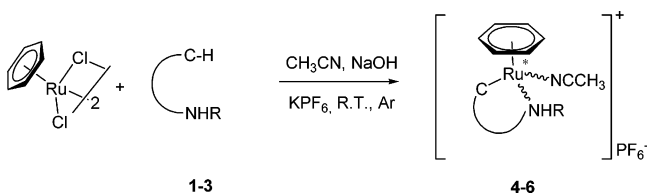
[‡] Service Commun des Rayons X.

(1) Sortais, J.-B.; Rittleng, V.; Voelklin, A.; Holuigue, A.; Smail, H.; Barloy, L.; Sirlin, C.; Verzijl, G. K. M.; Boogers, J. A. F.; de Vries, A. H. M.; de Vries, J. G.; Pfeffer, M. *Org. Lett.* 2005, 7, 1247–1250.

(2) Sortais, J.-B.; Barloy, L.; Sirlin, C.; de Vries, A. H. M.; de Vries, J. G.; Pfeffer, M. *Pure Appl. Chem.* 2006, 78, 457–462.

(3) In support of this assertion, we have found that cycloruthenation of (*R*)-*N*-benzyl(1-phenyl)ethylamine led to an intractable mixture of at least eight cycloruthenated species.

Scheme 1. Cycloruthenation Reaction



Solution NMR Analysis. As for other reported related complexes,⁴ evidence for the metalation of the aryl unit was provided by the ¹H NMR spectra of complexes **4–7**, which showed the disappearance of one aromatic proton of the corresponding amine. Furthermore, proton H^o in *ortho* position with regard to the Ru–C bond is deshielded, and it presents a strong NOE interaction with the η⁶-benzene ligand. The complexes display the usual pseudo-tetrahedral geometry of ruthenium half-sandwich complexes. In addition to the metal and carbon atoms (the latter with a fixed (*R*) configuration), the nitrogen atom is also a stereogenic center, so that four diastereomers with respective (*R*_{Ru},*R*_N), (*R*_{Ru},*S*_N), (*S*_{Ru},*R*_N), and (*S*_{Ru},*S*_N) configurations coexist in solution for each complex. The proportions of these diastereomers after crystallization as described in the Experimental Section are given in Table 1. However, other diastereomeric ratios can be obtained through recrystallization of these complexes (*vide infra*). Only the tridimensional structures of isomers whose proportion is superior to 20% (*viz.*, **4a**, **4b**, **5a**, **5b**, **6a**, **7a**, and **7b**) could be identified with the help of ¹H NOESY or ROESY NMR spectroscopy, the other isomers being too diluted to provide relevant NMR information.

The major isomers **a** of complexes **4**, **5**, and **7** have structural characteristics in common, and so do isomers **b**. They are represented in Schemes 3 and 4. Throughout the paper, the substituents of the nitrogen atom are distinguished by the letter “*m*” for the one that has been *ortho*-metalated and “*f*” as free for the unmetalated one. Key NOE contacts characteristic of 1,3-diaxial interactions are always observed between Me_{*m*} and η⁶-C₆H₆. This indicates that the configuration of the ruthenium atom is (*S*), and it excludes a λ conformation for the metallacycle.

The configuration of the nitrogen atom is established by NMR features affecting the free part of the amine ligand. Remarkably high values (11–12 Hz) have been measured for the ³J_{HH} coupling constant corresponding to the H–N–C_{*f*}–H unit (Table 2), either with isomers **a** or with isomers **b**. As for cyclometalated primary amines,⁴ we could use the Karplus-like relationship applied to H–N–C–H structural units.⁶ This value of ³J_{HH} shows that there is no free rotation around the N–C_{*f*} bond, but that it is frozen in a conformation where the H–N–C_{*f*}–H_{*f*} torsion angle is close to 180°, obviously for steric reasons (*vide infra*).

NOE cross-peaks detected between the signals of Me_{*f*} and those of η⁶-C₆H₆ provide evidence that isomers **a** of complexes **4**, **5**, and **7** present the *S*_N configuration (Scheme 3). This assertion is also supported by (i) the *cis* relative position of NH and Me_{*m*}, illustrated by a NOE cross-peak between their signals, and (ii) in the case of complex **7a**, a NOE interaction between Me_{*f*} and one methyl of the phosphine. The values of ³J_{HH} coupling constants applied to the H–N–C_{*m*}–H unit (Table 2) allow us to determine the conformation of the ruthenacycle with the help of Newman projections (Scheme 5). For isomers

4a and **5a**, this value is zero, in agreement with a torsion angle close to 90° and with a δ conformation; by contrast, the metallacycle of **7a** is rather planar according to the observed value of 3.5 Hz.

Conversely, the nitrogen atom of diastereoisomers **b** of complexes **4**, **5**, and **7** is (*R*) according to Me_{*f*}/Me_{*m*}, H_{*f*}/Me_{*m*}, and Me_{*f*}/H_{*m*} NOE cross-peaks (Scheme 4). This configuration is confirmed by a H16/η⁶-C₆H₆ NOE for complex **5b**, although the intensity of the cross-peak is rather low. The ³J_{HH} coupling constants for the H–N–C_{*m*}–H unit are all within 3–4 Hz (Table 2). This hints at a torsion angle close to 60° rather than 0° and, therefore, a marked δ (rather than planar) conformation, in which the free substituent on the nitrogen is uncongested in equatorial position. By comparison with isomers **a**, the η⁶-C₆H₆ proton signal of isomers **b** is shielded because of the proximity of the free phenyl or naphthyl group, with Δδ (=δ_{*b*} – δ_{*a*}) respective values of –0.44 (compound **4**), –0.83 (compound **5**), and –0.32 (compound **7**) ppm.

Concerning complex **6a**, its (*R*_{Ru}) configuration is demonstrated by a NOE between H7 and η⁶-C₆H₆, and its (*R*_N) configuration by NH/H7 and NH/η⁶-C₆H₆ NOEs (Scheme 6). H7 is coupled to NH with a constant of 7.8 Hz, which is rather high in comparison with other (*R*_N) isomers (*i.e.*, **4b**, **5b**, and **7b**, see Table 2); this militates in favor of a torsion angle close to zero and, thus, of a planar ruthenacycle.

It is noteworthy that in complexes **4**, **6**, and **7**, the *ortho* and *meta* ¹H and ¹³C{¹H} resonances of the free phenyl group are averaged, which means that it rotates freely at room temperature about the C–C bond. By contrast, several ¹H signals belonging to the free, voluminous naphthyl group of **5a** are broad at RT; we assume that this is the result of a slow equilibrium between two atropoisomers (see Supporting Information). The ¹H signals of **5b** are all narrow, indicating either that the orientation of the free substituent on the nitrogen atom is fixed or that it is rotating freely. However, examination of a molecular model of **5b** in agreement with NMR data suggests that the former hypothesis is true, because of several intramolecular steric clashes (see Supporting Information).

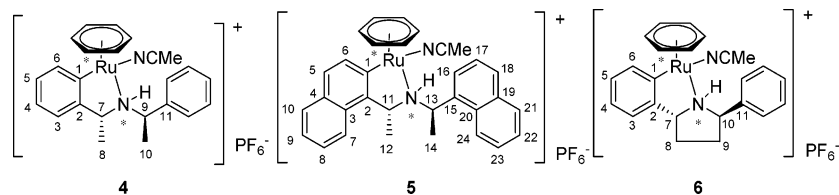
X-ray Analysis. Single crystals suitable for X-ray analysis were obtained for complexes **4**, **6**, and **7**. The isolated crystals of **4** and **6** contained respectively the (*S*_{Ru},*S*_N) (**4a**, Figure 1) and (*R*_{Ru},*R*_N) (**6a**, Figure 2) isomers, whereas two different kinds of crystals corresponding to the (*S*_{Ru},*R*_N) (**7a**, Figure 3) and (*S*_{Ru},*R*_N) (**7b**, Figure 4) isomers were obtained from a solution of **7**. The following measured bond distances fall within the expected range:⁷ Ru–(centroid of η⁶-C₆H₆) (1.71–1.75 Å); Ru–C_{aryl} (2.05–2.07 Å); Ru–N_{amine} (2.15–2.20 Å); Ru–P (2.33 Å); incidentally, the Ru–N_{amine} bond lengths are longer than in ruthenacyclic primary amines.

Overall, the conformations that have been deduced from ¹H NMR analysis in solution were also observed in the crystallographic structures. The five-membered ruthenacycles of complexes **4a** and **7b** present a δ envelope conformation. The ruthenium and carbon atoms are almost coplanar (Ru–C_{aryl}–C_{aryl}–C_{benzyl} torsion angle = 1–2°), and the nitrogen atom deviates from their plane with a N–C_{benzyl}–C_{aryl}–C_{aryl} ranging from 21° to 27°. As with primary amines, the Me_{*m*} group is axial, and the η⁶-C₆H₆ ligand pseudoaxial with centroid–Ru–C_{aryl}–C_{aryl} torsion angles of ca. 119°. By contrast, in complexes **6a** and **7a**, the ruthenacycle is virtually planar: deviations of the atoms of the five-membered cycle with regard to their mean plane are less than 0.05 Å.

(6) Fraser, R. R.; Renaud, R. N.; Saunders, J. K.; Wigfield, Y. Y. *Can. J. Chem.* **1973**, *51*, 2433–2437.

(7) Orpen, A. G.; Brammer, L.; Allen, F. H.; Kennard, O.; Watson, D. G.; Taylor, R. *J. Chem. Soc., Dalton Trans.* **1989**, S1–S83.

Chart 2. Half-Sandwich Ruthenium(II) Complexes



Scheme 2

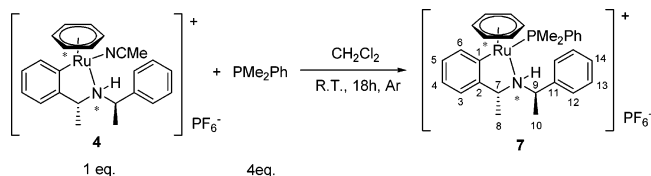
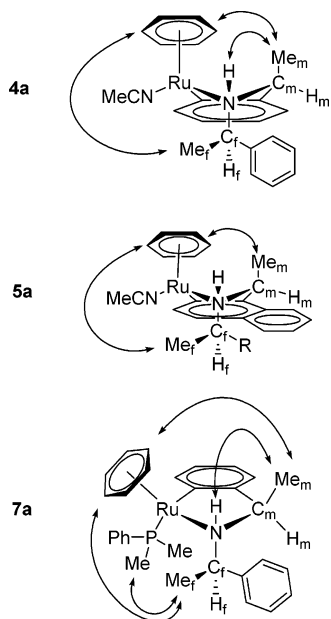


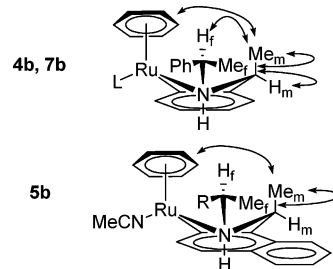
Table 1. Isomeric Repartition (in decreasing order) in Solution of Complexes 4–7 at RT

compound	proportion (%)			
	a	b	c	d
4 ^a	69	29	1	1
5 ^a	46	40	10	4
6 ^a	76	12	7	5
7 ^b	75	23	1	1

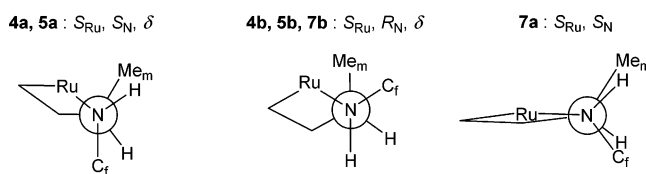
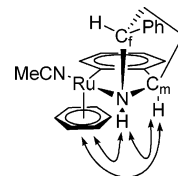
^a In CD₃CN. ^b In CD₂Cl₂.Scheme 3. Tridimensional Structure of the Diastereoisomer a (*S*_{Ru}, *S*_N configuration) of Complexes 4, 5 (*R* = C₁₀H₇) and 7^a

^a For the sake of clarity, the positive charges of the complexes have been omitted. Double arrows represent key NOE contacts. “m” stands for metalated and “f” stands for free.

It is noteworthy that the conformations of the free substituent on the nitrogen in complexes **4a**, **7a**, and **7b** reflect our NMR observations. This is highlighted by the value of the Ru–N–C_f–Me_f torsion angle, which is –62° in **4a**, –50° in **7a**, and 176° in **7b**; as a (coincidental) consequence, the NH and H_f proton are *anti*. These conformations are probably the result a balance between steric intramolecular repulsions involving various fragments of the complexes, i.e., the η⁶-C₆H₆ ligand, the fourth ligand (acetonitrile or phosphine), Me_m, and the substituents on C_f (aryl and Me_f). In (*S*_N)-**a** isomers, C_m and its

Scheme 4. Tridimensional Structure of the Diastereoisomer b (*S*_{Ru}, *R*_N configuration) of Complexes 4 (*L* = MeCN), 5 (*R* = C₁₀H₇), and 7 (*L* = PMe₂Ph)^a^a Double arrows represent key NOE contacts.Table 2. Coupling Constants ³J_{HCNH} in Complexes 4, 5, and 7

compound	coupling constant ³ J _{HH} (Hz)	
	HC _m NH	HC _f NH
4a	0.0	11.8
4b	3.7	11.9
5a	0.0	11 ^a
5b	3.6	11.8
7a	3.5	11.5
7b	4.0	11.8

^a ¹H NMR broad signal for H₉ proton.Scheme 5. Newman View of Complexes 4, 5, and 7 along the N–C_m BondScheme 6. Tridimensional Structure of Complex 6a^a^a Double arrows represent key NOE contacts.

substituents are in close proximity to the acetonitrile or phosphine ligand, which is *cis* with regard to the ruthenacycle. Therefore the bulky aryl group on C_m points away from this ligand; however it is still in a crowded position, as revealed by the restricted rotation of the naphthyl group of **5a** (*vide supra*). In the (*R*_N)-**b** isomers, C_m and its substituents are closer to the *cis*-positioned Me_m and to η⁶-C₆H₆, and therefore the bulkiest substituents (aryl and Me_f) are repelled away from them.

An indication of the strong steric conflict between the phosphine and the free substituent on the nitrogen in the structure of complex **7a** is the important difference between the N–Ru–P1 angle and the C16–Ru–P1 angle (12.4°). This

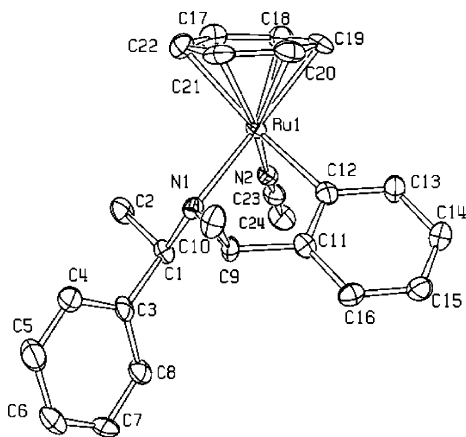


Figure 1. ORTEP style plot of compound **4a**. Thermal ellipsoids are drawn at the 50% probability level. Hydrogen atoms, PF_6^- anion, and CH_2Cl_2 are omitted for clarity. Selected bond lengths [\AA] and bond angles [deg]: Ru1–Centroid 1.718(8), Ru1–C12 2.057(6), Ru1–N2 2.063(6), Ru1–N1 2.185(5), C12–Ru1–N2 85.0(2), C12–Ru1–N1 79.4(2), N2–Ru1–N1 91.5(2), N1–Ru1–Centroid 129.4(2), C12–Ru1–Centroid 127.8(3).

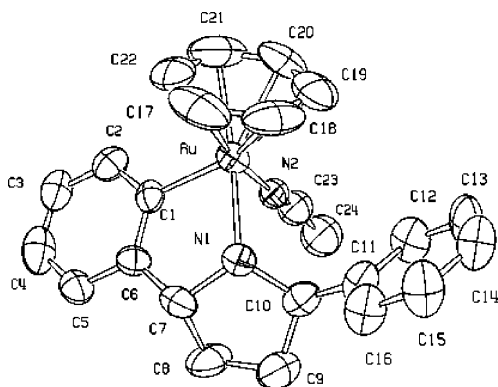


Figure 2. ORTEP style plot of compound **6a**. Thermal ellipsoids are drawn at the 50% probability level. The hydrogen atoms and the PF_6^- anion are omitted for clarity. The acetonitrile ligand is disordered on two positions; only one is depicted here. Selected bond lengths [\AA] and bond angles [deg]: Ru–Centroid 1.717(10), Ru–C1 2.066(6), Ru–N1 2.150(6), Ru–N2 2.155(12), C1–Ru–N1 79.4(3), C1–Ru–N2 81.9(4), N1–Ru–N2 85.7(4), N1–Ru–Centroid 129.3(5), C1–Ru–Centroid 129.3(5).

difference is much smaller (4.0°) in **7b**: indeed the amine is then less tilted away from the phosphine, as its free substituent is now *trans* to the phosphine with regard to the metallacycle. However, in **7b** the steric clash between $\eta^6\text{-C}_6\text{H}_6$ and the free benzylic substituent on the nitrogen is illustrated by a larger N–Ru–Centroid angle ($133.28(16)^\circ$) than in **7a** ($127.39(15)^\circ$).

In the X-ray structure of **6a**, we notice that N1, C7, C8, and C10 are coplanar (deviation $<0.04 \text{ \AA}$ from mean plane). The conformation of the pyrrolidine ring is envelope, and the unmetalated phenyl group occupies a sterically stabilized equatorial position.⁸ As in ruthenacyclic primary amines, the phosphine phenyl group of complexes **7a** and **7b** is located below the ruthenacycle ($\text{C}_{\text{ipso}}\text{-P-Ru-N}$ torsion angles are respectively -22° and -12°).

Configurational Stability. We determined the relative proportion of each isomer of compound **4** by ^1H NMR at various temperatures ranging from 233 to 313 K in acetonitrile, letting

(8) ^1H NMR analysis of the pyrrolidine ring reveals a conformation close to that determined by the X-ray diffraction study (see Supporting Information).

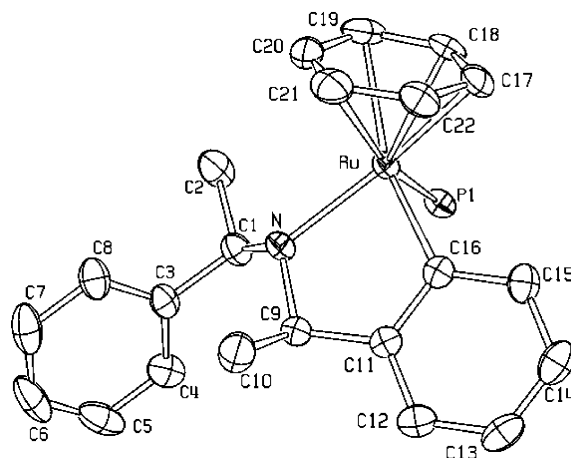


Figure 3. ORTEP style plot of compound **7a**. Thermal ellipsoids are drawn at the 50% probability level. Hydrogen atoms, PF_6^- anion, CH_2Cl_2 , and substituents of PMe_2Ph are omitted for clarity. Selected bond lengths [\AA] and bond angles [deg]: Ru–Centroid 1.747(4), Ru–C16 2.048(3), Ru–N 2.196(3), Ru–P1 2.3354(9), C16–Ru–N 80.33(11), C16–Ru–P1 84.01(8), N–Ru–P1 96.41(7), N–Ru–Centroid 127.39(15), C16–Ru–Centroid 126.92(15).

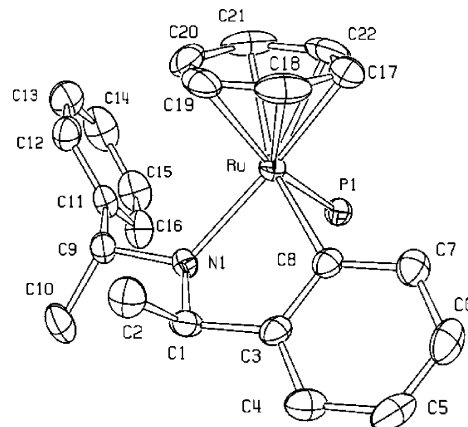


Figure 4. ORTEP style plot of compound **7b**. Thermal ellipsoids are drawn at the 50% probability level. Hydrogen atoms, PF_6^- anion, and substituents of PMe_2Ph are omitted for clarity. Selected bond lengths [\AA] and bond angles [deg]: Ru–Centroid 1.752(4), Ru–C8 2.072(3), Ru–N1 2.190(2), Ru–P1 2.3339(8), C8–Ru–N1 77.85(11), C8–Ru–P1 87.03(9), N1–Ru–P1 90.98(8), N1–Ru–Centroid 133.28(16), C8–Ru–Centroid 124.59(16).

the mixture stabilize for 15 min at each temperature, and did not notice any modification. Moreover, leaving the sample at 233 K for a week does not change the ratios either. Since the (S_{Ru}) diastereoisomers **4a** and **4b** are overwhelmingly major (respectively 69% and 29%, see Table 1), we cannot conclude concerning the configurational stability at the metal. However, different recrystallized samples of **4** can present dramatically altered **4a/4b** ratios (e.g., 85:15) that remain unchanged within hours at RT. All these observations suggest that **4a** and **4b** do not exchange and that, as with primary amines, there would be no fluxional process in which the Ru–N bond would be broken. Similarly, complex **7a** has been almost isolated pure (**7a/7b** ratio = 95:5) by fractional crystallization from a dichloromethane solution, and it has been checked that a solution of this sample in CD_2Cl_2 is stable (i.e., this ratio remains unchanged) within 24 h; therefore complex **7** is configurationally stable at nitrogen on a laboratory time scale.

Concluding Remarks

Good correlations between NMR and X-ray analyses of ruthenacyclic secondary amines were found concerning their three-dimensional structures, i.e., their configurations and conformations. A remarkable characteristic that these complexes share with homologous primary amines, and not with tertiary amines, is the fact that an (S_{Ru}) configuration is generally associated with a δ conformation, and a (R_{Ru}) configuration with a λ conformation, with a pseudoaxial η^6 -benzene ligand. However, sometimes steric factors force the metallacycle into a planar rather than envelope conformation (complexes **6a** and **7b**). The (S_{Ru}) isomers of complexes **4**, **5**, and **7** are the most stable thermodynamically, whereas for complex **6** the (R_{Ru}, R_N) isomer (**6a**) is the most stable one.

The compounds **4**–**6** are active catalysts precursors for the asymmetric transfer hydrogenation of ketones.^{1,2} We may assume that this reaction proceeds via the bifunctional mechanism proposed by Noyori et al.,⁹ involving a Ru compound having a hydride unit instead of the ancillary ligand MeCN or PMe₂Ph. Among the four isomers of a given ruthenacyclic secondary amine, two [(S_{Ru}, R_N) and (R_{Ru}, S_N)] bear a NH vector that is roughly parallel with the Ru–L vector, and the two others [(S_{Ru}, S_N) and (R_{Ru}, R_N)] display a NH vector that is not; for instance, the H–N–Ru–P torsion angle is ca. 6° in the X-ray structure of (S_{Ru}, R_N)-**7b** and –161° in the structure of (S_{Ru}, S_N)-**7a**. According to the bifunctional mechanism operating through a six-membered transition state, the (S_{Ru}, R_N) and (R_{Ru}, S_N) ruthenium hydrides should be active catalytic species and the (S_{Ru}, S_N) and (R_{Ru}, R_N) ruthenium hydrides should not. It is noteworthy that the (S_{Ru}, R_N) and (R_{Ru}, S_N) isomers studied in this paper are all minor; therefore we may assume that catalytically active hydrides are minor species.

Experimental Section

Experiments were carried out under an argon atmosphere using a vacuum line. Diethyl ether and pentane were distilled over sodium and benzophenone; dichloromethane and acetonitrile, over calcium hydride under argon immediately before use. Column chromatography was carried out on Merck aluminum oxide 90 standardized. The following commercial reagents were used as received. Aldrich: (+)-bis[(*R*)-(α-methylbenzyl)]amine 99%, (–)-bis[(*R*)-(1-naphthyl)ethyl]amine hydrochloride 98%, 1,3-cyclohexadiene, sodium hydroxide. Lancaster: potassium hexafluorophosphate. Avocado: dimethylphenylphosphine. The compounds listed hereafter were synthesized following reported procedures: [Ru(η^6 -C₆H₆)Cl₂]₂,¹⁰ (*2R,5R*)-2,5-diphenylpyrrolidine.¹¹ The NMR spectra were obtained at room temperature (unless otherwise indicated) on Bruker spectrometers. ¹H NMR spectra were recorded at 300.13 MHz (AC-300), 400.13 MHz (AM-400), or 500.13 MHz (ARX-500) and referenced to SiMe₄. ¹³C{¹H} NMR spectra (broadband decoupled) were recorded at 75.48 MHz (AC-300), 100.62 MHz (AM-400), or 125.76 MHz (ARX-500) and referenced to SiMe₄. ³¹P{¹H} NMR spectra (broadband decoupled) were recorded at 121.51 MHz (AC-300) or 202.46 MHz (ARX-500) and referenced to 85% aqueous H₃PO₄. For variable-temperature spectra, the probe temperature was controlled (±1 K) by a B-VT 2000 unit calibrated with a methanol NMR tube. The NMR assignments were supported by COSY, NOESY, or ROESY spectra or irradiations for ¹H NMR, and DEPT-135° and/or HSQC, HMQC, and HMBC spectra for ¹³C{¹H} NMR. For the adopted numbering scheme, see Chart 2

(9) Noyori, R.; Masashi, Y.; Hashiguchi, S. *J. Org. Chem.* **2001**, *66*, 7931–7944.

(10) Zelonka, R. A.; Baird, M. C. *Can. J. Chem.* **1972**, *50*, 3063–3072.

(11) Chong, J. M.; Clarke, I. S.; Koch, I.; Olbach, P. C.; Taylor, N. J. *Tetrahedron: Asymmetry* **1995**, *6*, 409–418.

and Scheme 3. Multiplicity: s = singlet, d = doublet, t = apparent triplet, q = quadruplet, sept = septuplet, m = multiplet, br = broad signal, app = apparent. ES-MS spectra and elemental analyses were carried out by the corresponding facilities at the Institut de Chimie, Université Louis Pasteur, Strasbourg, and at the Service Central d'Analyse du CNRS, Vernaison. Some diastereoisomers of our compounds cocrystallized with solvent molecules, i.e., CH₂Cl₂ (see X-ray structures of **4a** and **7a**) or CH₃CN. This led to mixtures of diastereoisomers whose molecular formulas included fractions of solvents. The presence of solvents was checked by ¹H NMR, and the amount was found approximately proportional to the diastereoisomers ratio.

[(η^6 -C₆H₆)Ru(C₆H₄-2-(*R*)-CH(CH₃)NH-(*R*)-CH(CH₃)-C₆H₅)-(NCCH₃)](PF₆) (**4**). To a suspension of [Ru(η^6 -C₆H₆)Cl₂]₂ (2.18 g, 4.36 mmol), NaOH (0.35 g, 8.75 mmol), and KPF₆ (3.2 g, 17.39 mmol) in CH₃CN (65 mL) was added the amine **1** (0.98 g, 4.36 mmol), and the mixture was stirred at 20 °C under argon during 72 h. The resulting dark yellow suspension was filtered over Celite, concentrated in vacuo, and filtered over standardized Al₂O₃ (12 × 3 cm) using CH₃CN as eluent. A yellow fraction was collected, concentrated *in vacuo* to ca. 5 mL, and stirred with 20 mL of hexane during 2 h, in order to extract the residual free amine. The acetonitrile layer was concentrated *in vacuo*, the yellow residue was then redissolved in a minimum of CH₂Cl₂, and a yellow solid precipitated (1.79 g, 65% yield) upon addition of *n*-pentane. Anal. Calcd for C₂₄H₂₇F₆N₂PRu, 2/3 CH₂Cl₂: C 45.85, H 4.42, N 4.34. Found: C 45.55, H 4.48, N 4.13. ¹H NMR (300 MHz, CD₃CN, 298 K): **4a** (69%), δ 7.70 (dd, 1H, H₆, ³J_{HH} = 7.5 Hz, ⁴J_{HH} = 0.9 Hz), 7.54–7.34 (m, 5H, H_{ar}), 7.01 (td, 1H, H₅, ³J_{HH} = 7.3 Hz, ⁴J_{HH} = 1.6 Hz), 6.86 (td, 1H, H₄, ³J_{HH} = 7.4 Hz, ⁴J_{HH} = 1.2 Hz), 6.67 (dd, 1H, H₃, ³J_{HH} = 7.4 Hz, ⁴J_{HH} = 1.3 Hz), 5.74 (s, 6H, η^6 -C₆H₆), 5.07 (br d, 1H, NH, ³J_{HH} = 11 Hz), 3.62 (q, 1H, H₇, ³J_{HH} = 6.8 Hz), 3.43 (dq, 1H, H₉, ³J_{HH} = 11.8 Hz, ³J_{HH} = 6.6 Hz), 1.80 (d, 3H, H₁₀, ³J_{HH} = 6.9 Hz), 0.92 (d, 3H, H₈, ³J_{HH} = 6.9 Hz); **4b** (29%), δ 7.62 (dd, 1H, H₆, ³J_{HH} = 7.3 Hz, ⁴J_{HH} = 1.3 Hz), 7.54–7.34 (m, 5H, H_{ar}), 7.07 (dd, 1H, H₃, ³J_{HH} = 7.1 Hz, ⁴J_{HH} = 1.8 Hz), 6.92–7.02 (m, 2H, H₄ + H₅), 5.27 (s, 6H, η^6 -C₆H₆), 4.47 (br, 1H, NH), 4.42 (qd, 1H, H₇, ³J_{HH} = 6.5 Hz, ³J_{HH} = 3.7 Hz), 4.37 (dq, 1H, H₉, ³J_{HH} = 11.9 Hz, ³J_{HH} = 6.4 Hz), 1.51 (d, 3H, H₁₀, ³J_{HH} = 6.0 Hz), 1.23 (d, 3H, H₈, ³J_{HH} = 6.3 Hz) ppm. ¹³C{¹H} NMR (125 MHz, CD₃CN, 273 K): **4a**, δ 164.7 (C1), 152.4 (C2), 143.0 (C11), 139.8 (C6), 129.7 (2C, CH_{ar}), 128.7 (2C, CH_{ar}), 127.6 (CH_{ar}), 127.0 (C5), 124.1 (C4), 122.1 (C3), 87.7 (η^6 -C₆H₆), 66.1 (C7), 62.7 (C9), 25.5 (C10), 23.8 (C8); **4b**, selected data, δ 87.4 (η^6 -C₆H₆).

[(η^6 -C₆H₆)Ru(C₁₀H₆-2-(*R*)-CH(CH₃)NH-(*R*)-CH(CH₃)-C₁₀H₇)-(NCCH₃)](PF₆) (**5**). The commercial amine hydrochloride (200 mg, 0.55 mmol) was dissolved in water with NaOH and extracted with Et₂O prior to use. After drying over Na₂SO₄, the organic layer was evaporated to afford the pure amine **2**. The procedure was then the same as for **4**: [Ru(η^6 -C₆H₆)Cl₂]₂ (274 mg, 0.55 mmol), NaOH (44 mg, 1.1 mmol), KPF₆ (405 mg, 2.2 mmol), CH₃CN (10 mL), and the chiral amine **2** gave after 21 days **5** (90 mg, 23% yield). Anal. Calcd for C₃₂H₃₁F₆N₂PRu, 2/3 CH₂Cl₂: C 52.58, H 4.37, N 3.75. Found: C 52.72, H 4.46, N 4.04. ES-MS: *m/z* (%) 504.0488 (100) [M – CH₃CN]⁺. ¹H NMR (500 MHz, CD₃CN, 298 K): **5a** (46%), δ 8.05 (br, 1H, H₁₆), 7.98 (d, 1H, H₆, ³J_{HH} = 8.5 Hz), 7.98–7.94 (m, 2H, H₁₈ + H₂₁), 7.78–7.73 (m, 2H, H₁₀ + H₁₇), 7.60–7.55 (m, 1H, H₅), 7.46–7.40 (m, 2H, H₂₂ + H₂₄), 7.16 (ddd, 1H, H₉, ³J_{HH} = 8.0 Hz, ³J_{HH} = 6.5 Hz, ⁴J_{HH} = 1.0 Hz), 7.12–7.07 (br, 1H, H₂₃), 6.94 (br t, 1H, H₈, ³J_{HH} = 8 Hz), 6.57 (br d, 1H, H₇, ³J_{HH} = 8 Hz), 5.86 (s, 6H, η^6 -C₆H₆), 5.39 (br d, 1H, NH, ³J_{HH} = 11 Hz), 4.46 (br dq, 1H, H₁₃, ³J_{HH} = 11 Hz, ³J_{HH} = 7 Hz), 4.32 (q, 1H, H₁₁, ³J_{HH} = 6.7 Hz), 1.98 (d, 3H, H₁₄, ³J_{HH} = 6.5 Hz), 1.03 (d, 3H, H₁₂, ³J_{HH} = 7.0 Hz); **5b** (40%), δ 8.44 (d, 1H, H₂₄, ³J_{HH} = 8.5 Hz), 8.09 (d, 1H, H₂₁, ³J_{HH} = 8.5 Hz), 8.02 (m, 1H, H₁₈), 7.88–7.84 (m, 2H, H₇ + H₁₀), 7.84 (d, 1H, H₆,

Table 3. Crystal Data and Structure Refinement for 4a, 6a, 7a, and 7b

	4a	6a	7a	7b
formula	C ₂₄ H ₂₆ F ₆ N ₂ PRu·CH ₂ Cl ₂	C ₂₄ H ₂₅ F ₆ N ₂ PRu	C ₃₀ H ₃₅ F ₆ NP ₂ Ru·CH ₂ Cl ₂	C ₃₀ H ₃₅ F ₆ NP ₂ Ru
fw	673.43	587.50	771.53	686.60
cryst syst	orthorhombic	orthorhombic	orthorhombic	orthorhombic
space group	P2 ₁ 2 ₁ 2 ₁	P2 ₁ 2 ₁ 2 ₁	P2 ₁ 2 ₁ 2 ₁	P2 ₁ 2 ₁ 2 ₁
a, Å	10.1140(2)	8.43300(10)	10.38700(10)	12.8140(2)
b, Å	14.1300(3)	10.1720(2)	11.30700(10)	13.3690(2)
c, Å	19.0980(4)	28.4470(6)	28.1380(4)	17.0310(3)
V, Å ³	2729.31(10)	2440.20(8)	3304.69(6)	2917.59(8)
Z	4	4	4	4
ρ _{calcd} , g/cm ³	1.639	1.599	1.551	1.563
μ, mm ⁻¹	0.888	0.769	0.790	0.707
F(000)	1356	1184	1568	1400
cryst size, mm ³	0.15 × 0.12 × 0.10	0.14 × 0.14 × 0.12	0.12 × 0.10 × 0.10	0.12 × 0.10 × 0.08
θ range, deg	2.6 to 30.0	2.13 to 30.04	1.45 to 30.03	2.39 to 30.03
index ranges	-14 ≤ h ≤ 14 -19 ≤ k ≤ 19 -26 ≤ l ≤ 26	-11 ≤ h ≤ 7 -14 ≤ k ≤ 11 -40 ≤ l ≤ 20	-14 ≤ h ≤ 14 -15 ≤ k ≤ 15 -39 ≤ l ≤ 39	-18 ≤ h ≤ 18 -18 ≤ k ≤ 18 -23 ≤ l ≤ 23
no. of reflns colld	7939	17 055	9649	8470
no. of indep colld/R _{int}	7939/0.05	7063/0.0454	7393/0.03	6620/0.04
completeness to θ _{max} , %	99.7	99.6	99.9	99.9
no. of refined params	337	304	388	361
GOF (F ²)	1.001	1.052	1.042	1.069
R1(F) (I > 2σ(I))	0.0889	0.0668	0.0424	0.0436
wR2(F ²) (I > 2σ(I))	0.1805	0.1724	0.0891	0.0933
absolute struct param	0.04(5)	0.02(7)	-0.03(3)	-0.05(3)
largest diff peak/hole, e ⁻ Å ⁻³	1.64/-0.99	0.952/-0.907	0.982/-1.095	1.088/-0.948

³J_{HH} = 8.0 Hz), 7.78–7.73 (m, 1H, H23), 7.70–7.65 (m, 2H, H17 + H22), 7.60–7.55 (m, 2H, H5 + H16), 7.49 (ddd, 1H, H8, ³J_{HH} = 8.5 Hz, ³J_{HH} = 6.5 Hz, ³J_{HH} = 1.0 Hz), 7.37 (ddd, 1H, H9, ³J_{HH} = 8.5 Hz, ³J_{HH} = 7.0 Hz, ³J_{HH} = 1.0 Hz), 5.31 (dq, 1H, H13, ³J_{HH} = 11.8 Hz, ³J_{HH} = 6.5 Hz), 5.30 (qd, 1H, H11, ³J_{HH} = 6.5 Hz, ³J_{HH} = 3.6 Hz), 5.03 (s, 6H, η⁶-C₆H₆), 4.89 (br d, 1H, NH, ³J_{HH} = 11 Hz), 1.76 (d, 3H, H14, ³J_{HH} = 6.5 Hz), 1.53 (d, 3H, H12, ³J_{HH} = 6.5 Hz); **5c** (10%) selected data, 5.91 (s, 6H, η⁶-C₆H₆), 5.67 (q, 1H, H13, ³J_{HH} = 6.5 Hz), 5.24 (q, 1H, H11, ³J_{HH} = 6.5 Hz), 1.22 (d, 3H, H12, ³J_{HH} = 6.5 Hz). ¹³C{¹H} NMR (125 MHz, CD₃CN, 300 K): **5a**, δ 164.9 (C1), 145.6 (C2), 139.3 (C15), 138.9 (C6), 132.4 (C4), 130.8 (C20), 129.9 (C18), 129.4 (C21), 129.2 (C3), 129.0 (C10), 127.4 (C23), 126.9 (C24), 126.6 (C5), 126.5 (C17), 126.4 (C19), 126.1 (C8), 124.2 (C16), 124.1 (C9), 123.1 (C7), 122.7 (C22), 88.3 (η⁶-C₆H₆), 64.6 (C11), 56.4 (C13), 25.5 (C14), 22.3 (C12); **5b**, δ 163.8 (C1), 145.6 (C2), 141.4 (C15), 139.0 (C6), 134.7 (C20), 132.5 (C2), 130.2 (C21), 129.4 (C10), 129.2 (C18), 128.9 (C3), 128.1 (C23), 127.1 (C19), 126.8 (C8), 126.5 (C5), 126.2 (C22), 126.1 (C17), 125.1 (C16), 124.4 (C9), 124.0 (C7), 123.0 (C24), 87.4 (η⁶-C₆H₆), 62.9 (C11), 57.9 (C13), 22.2 (C14), 17.8 (C12); **5c**, selected data, 162.5 (C1), 143.6 (C2), 89.6 (η⁶-C₆H₆), 73.4 (C11), 73.2 (C13), 23.2 (C12), 22.6 (C14).

[(η⁶-C₆H₆)Ru(κ²-C,N-(2R,5R)-2,5-diphenylpyrrolidine)(NCCCH₃)](PF₆) (**6**). The followed procedure was the same as for **4**: [Ru(η⁶-C₆H₆)Cl₂]₂ (100 mg, 0.2 mmol), NaOH (16 mg, 0.4 mmol), KPF₆ (150 mg, 0.8 mmol), CH₃CN (4 mL), and the chiral amine **3** (45 mg, 0.2 mmol) gave after 3 days **6** (100 mg, 85% yield). Anal. Calcd for C₂₄H₂₅F₆N₂PRu, 1/3 CH₃CN: C 49.28, H 4.36, N 5.44. Found: C 48.90, H 4.71, N 5.61. ¹H NMR (500 MHz, CD₃CN, 300 K): **6a** (76%), δ 7.73 (dd, 1H, H6, ³J_{HH} = 7.1 Hz, ⁴J_{HH} = 1.5 Hz), 7.50–7.56 (m, 5H, H_{ar}), 7.01 (m, 1H, H4), 6.99 (td, 1H, H5, ³J_{HH} = 7.0 Hz, ⁴J_{HH} = 1.5 Hz), 6.90 (d, 1H, H3, ³J_{HH} = 6.5 Hz), 6.17 (br, 1H, NH), 5.32 (s, 6H, η⁶-C₆H₆), 4.62 (app q, 1H, H7, ³J_{HH} = 7.8 Hz), 3.84 (td, 1H, H10, ³J_{HH} = 11.0 Hz, ³J_{HH} = 5.5 Hz), 2.57 (m, 1H, H8), 2.22 (m, 1H, H9), 2.01 (m, 1H, H9), 1.85 (m, 1H, H8); **6b**, selected data (12%), δ 7.92 (d, 1H, H6, ³J_{HH} = 7.5 Hz), 5.34 (s, 6H, η⁶-C₆H₆); **6c**, selected data (7%), δ 7.97 (d, 1H, H6, ³J_{HH} = 7.0 Hz), 5.51 (s, 6H, η⁶-C₆H₆); **6d**, selected data (5%), δ 8.13 (d, 1H, H6, ³J_{HH} = 7.5 Hz), 5.19 (s, 6H, η⁶-C₆H₆). ¹³C{¹H} NMR (125 MHz, CD₃CN, 300 K): **6a**, δ 163.7 (C1), 152.7 (C2), 139.9 (C6), 139.6 (C11), 129.8 (2C, CH_{ar}), 129.2 (CH_{ar}), 128.2 (2C, CH_{ar}), 127.1 (C4), 124.7 (C5), 123.0 (C3), 87.9 (η⁶-C₆H₆), 73.1 (C7), 69.1 (C10), 37.5 (C9), 33.6 (C8).

[(η⁶-C₆H₆)Ru(C₆H₄-2-(R)-CH(CH₃)NH-(R)-CH(CH₃)-C₆H₅)-(P(CH₃)₂Ph)](PF₆) (**7**). A yellow solution of **4** (100 mg, 0.17 mmol) was stirred with P(CH₃)₂Ph (97 μL, 0.68 mmol) in CH₂Cl₂ (5 mL) for 18 h at room temperature. The resulting reaction mixture was dried *in vacuo* and washed with *n*-pentane (3 × 5 mL) to remove excess P(CH₃)₂Ph. The yellow residue was then redissolved in a minimum of CH₂Cl₂ (1 mL), and a yellow solid (90 mg, 76% yield) precipitated upon addition of *n*-pentane. Anal. Calcd for C₃₀H₃₅F₆-NP₂Ru, 3/4 CH₂Cl₂: C, 49.22; H, 4.90; N, 1.87. Found: C, 49.28; H, 4.90; N, 1.82. ³¹P{¹H} NMR (121 MHz, CD₂Cl₂, 300 K): **7a**, δ 5.53 (s, P(CH₃)₂Ph), -148.80 (septuplet, ¹J_{PF} = 709 Hz); **7b**, δ 9.74 (s, P(CH₃)₂Ph), -148.80 (sept, ¹J_{PF} = 709 Hz). ¹H NMR (300 MHz, CD₂Cl₂, 300 K): **7a** (75%), δ 7.45 (dd, 1H, H_p, ³J_{HH} = 7.5 Hz, ⁴J_{HH} = 1.5 Hz), 7.40 (dt, 1H, H6, ³J_{HH} = 6.3 Hz, ⁴J_{HH} = ⁴J_{HP} = 1.5 Hz), 7.36–7.26 (m, 5H, H_m + H13 + H14), 7.06–6.94 (m, 4H, H4 + H5 + H12), 6.81–6.76 (m, 2H, H_o), 6.58 (m, 1H, H3), 5.82 (d, 6H, η⁶-C₆H₆, ³J_{HP} = 0.9 Hz), 4.44 (br d, 1H, NH, ³J_{HH} = 11 Hz), 3.37 (qd, 1H, H7, ³J_{HH} = 6.6 Hz, ³J_{HH} = 3.3 Hz), 2.81 (dq, 1H, H9, ³J_{HH} = 11.5 Hz, ³J_{HH} = 6.9 Hz), 2.04 (d, 3H, P(CH₃)₂-Ph, ²J_{HP} = 8.7 Hz), 1.46 (d, 3H, H10, ³J_{HH} = 6.9 Hz), 1.42 (d, 3H, P(CH₃)₂Ph, ²J_{HP} = 9.6 Hz), 0.79 (d, 3H, H8, ³J_{HH} = 6.6 Hz); **7b**, selected data (23%), 5.50 (d, 6H, η⁶-C₆H₆, ³J_{HP} = 0.9 Hz), 3.99 (qd, 1H, H7, ³J_{HH} = 6.4 Hz, ³J_{HH} = 4.2 Hz), 3.91 (dq, 1H, H9, ³J_{HH} = 11.8 Hz, ³J_{HH} = 6.3 Hz), 2.98 (br d, 1H, NH, ³J_{HH} = 11 Hz), 1.74 (d, 3H, P(CH₃)₂Ph, ²J_{HP} = 9.0 Hz), 1.51 (d, 3H, P(CH₃)₂-Ph, ²J_{HP} = 9.9 Hz), 1.29 (d, 3H, H8, ³J_{HH} = 6.6 Hz), 1.18 (d, 3H, H10, ³J_{HH} = 6.6 Hz). ¹³C{¹H} NMR (75 MHz, CD₂Cl₂, 300 K): **7a**, δ 154.5 (s, C1), 140.4 (d, C2, ³J_{CP} = 5 Hz), 140.2 (s, C11), 135.8 (d, C_i, ¹J_{CP} = 40 Hz), 130.8 (d, C_p, ⁴J_{CP} = 2 Hz), 130.5 (d, C_o, ²J_{CP} = 8 Hz), 129.2 (s, 3C, C13 + C14), 129.0 (d, C_m, ³J_{CP} = 9 Hz), 128.9 (s, C6), 127.9 (s, 2C, C12), 126.4 (s, C4 or C5), 124.2 (s, C5 or C4), 123.4 (s, C3), 91.3 (d, η⁶-C₆H₆, ²J_{CP} = 3 Hz), 66.1 (s, C7), 64.8 (d, C9, ³J_{CP} = 6 Hz), 25.5 (s, C10), 25.0 (s, C8), 19.0 (d, P(CH₃)₂Ph, ¹J_{CP} = 31 Hz), 17.6 (d, P(CH₃)₂Ph, ¹J_{CP} = 37 Hz); **7b**, selected data, δ 90.5 (d, η⁶-C₆H₆, ²J_{CP} = 3 Hz).

X-ray Crystallography. Single crystals suitable for X-ray diffraction analysis were obtained by slow diffusion of *n*-hexane into a saturated solution of **4** in CH₂Cl₂ (**4a**), by slow diffusion of Et₂O into a saturated solution of **6** in CH₃NO₂ (**6a**), or by slow diffusion of *n*-pentane into a saturated solution of **7** in CH₂Cl₂ (**7a** and **7b**). The X-ray data were collected on a KappaCCD diffractometer with Mo Kα graphite-monochromated radiation (λ = 0.71073 Å) at 173 K. Details of data collection parameters and

refinement results are listed in Table 3. The structures were solved using direct methods. Hydrogen atoms were introduced as fixed contributors at calculated positions ($C-H = 0.95 \text{ \AA}$, $B(H) = 1.3B_{\text{eqv}}$). Final difference maps revealed no significant maxima. All calculations were done using the SHELXL-97 package.¹²

Acknowledgment. We thank DSM (N.L.) and the Ministère de l'Éducation Nationale (F) for fellowships (to N.P. and

(12) Sheldrick, M. *SHELXL-97, Program for crystal structure refinement*; University of Göttingen: Germany, 1997.

J.-B.S., respectively) and the CNRS for partial support of this work. We thank one of the referees for valuable suggestions.

Supporting Information Available: Structural data of complexes **4a**, **6a**, **7a**, and **7b** and figures of the equilibrium between rotamers of **5** and of the conformation of the pyrrolidine ring in complex **6a** in PDF format. Crystallographic data in CIF format for **4a**, **6a**, **7a**, and **7b**. These materials are available free of charge via the Internet at <http://pubs.acs.org>.

OM060974L